Available online at www.sciencedirect.com
SCIENCE DIRECT
Journal of Power Sources 156 (2006) 662–666
JOURNAL OF POWER SOURCES
www.elsevier.com/locate/jpowsour

Development of high-capacity nickel-metal hydride batteries using superlattice hydrogen-absorbing alloys

Shigekazu Yasuoka [a,*], Yoshifumi Magari [a], Tetsuyuki Murata [a], Tadayoshi Tanaka [a], Jun Ishida [a], Hiroshi Nakamura [a], Toshiyuki Nohma [a], Masaru Kihara [b], Yoshitaka Baba [b], Hirohito Teraoka [b]

[a] *Mobile Energy Company, Sanyo Electric Co. Ltd., 7-3-2, Ibukidai-higashimachi Nishi-ku, Kobe, Hyogo 651-2242, Japan*
[b] *Sanyo Energy Twicell Co. Ltd., 307-2 Koyagimachi, Takasaki, Gunma 370-0071, Japan*

Received 20 April 2005; received in revised form 12 May 2005; accepted 13 May 2005
Available online 22 July 2005

Abstract

New R–Mg–Ni (R: rare earths) superlattice alloys with higher-capacity and higher-durability than the conventional Mm–Ni alloys with $CaCu_5$ structure have been developed. The oxidation resistibility of the superlattice alloys has been improved by optimizing the alloy composition by such as substituting aluminum for nickel and optimizing the magnesium content in order to prolong the battery life. High-capacity nickel-metal hydride batteries for the retail market, the Ni-MH2500/900 series (AA size type 2500 mAh, AAA size type 900 mAh), have been developed and commercialized by using an improved superlattice alloy for negative electrode material.

Keywords: Nickel metal hydride battery; Hydrogen-absorbing alloy; Superlattice

1. Introduction

The retail market for nickel-metal hydride (Ni-MH) rechargeable batteries is expanding year by year as the market for such devices as digital still cameras continues to grow. Battery capacity is also steadily increasing, directly reflecting the demands for longer playing capabilities of such digital devices after charging them. However, it now appears to be difficult to increase battery capacity from current levels with such conventional materials as Mm–Ni (Mm: mischmetal) hydrogen-absorbing alloys with $CaCu_5$ structure.

To further increase battery capacity, a new material that can be substituted for conventional materials needs to be developed. It is reported that new R–Mg–Ni (R: rare earths) hydrogen-absorbing alloys with superlattice structure have been developed [1]. These alloys exhibited good electrochemical performance, such as a higher electrochemical capacity of 410 mAh g^{-1} at maximum, which was approximately 30% higher than the Mm–Ni alloys. It is also reported that the alloys showed good cycleability during a few tens of charge/discharge cycles in a three-electrode test cell. In spite of such good initial performance in a three-electrode test cell, the performance of the alloys in a practical battery has not been disclosed.

In this work, we elucidated the issues concerning battery life when using R–Mg–Ni alloys as the anode material and improved the alloys to achieve high-capacity and sufficient durability and eventually developed higher capacity batteries.

2. Experimental

Alloy ingots were prepared with high-frequency induction melting and then annealed at 900–950 °C in an argon atmosphere. The alloy ingots were crushed, ground into powder, and then sieved through a 100 mesh. The particle size of the alloy powders measured with a laser diffraction particle size

* Corresponding author. Tel.: +81 78 993 1129; fax: +81 78 993 1094.
E-mail address: yasuoka1@sm.energy.sanyo.co.jp (S. Yasuoka).

0378-7753/$ – see front matter © 2005 Elsevier B.V. All rights reserved.
doi:10.1016/j.jpowsour.2005.05.054

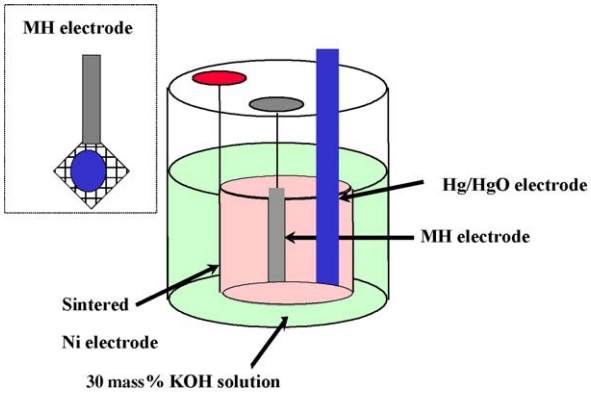

Fig. 1. Three-electrode test cell.

analyzer (Shimadzu SALD 2000) was approximately 65 μm. The crystal structure was analyzed with X-ray powder diffractometry (XRD) using Rigaku Model RINT2000. The XRD equipment was operated at 40 kV tube voltage and 40 mA tube current using Cu Kα radiation.

The discharge capacity of the hydrogen-absorbing alloys was measured using a three-electrode test cell, as shown in Fig. 1. The hydrogen-absorbing alloy (MH) electrode was assembled by mixing alloy and nickel powders (INCO type-255) at a weight ratio of 1:3 and compressing the mixture under pressure of 150 MPa. The size of the formed pellet was about 10 mm in diameter and 2 mm thick. The pellet was wrapped with a nickel net and welded with nickel lead. The three-electrode test cell consisted of the prepared working hydrogen-absorbing alloy electrode, a counter electrode of sintered nickel electrode, an Hg/HgO reference electrode, and electrolyte of a 30 mass% KOH aqueous solution. The three-electrode test cell was charged at 150 mA g^{-1} for 2 h and 50 min and discharged at 150 mA g^{-1} until the negative electrode potential reached −0.7 V with respect to the Hg/HgO electrode. The electrochemical capacity was evaluated with maximum capacity during the first eight charge/discharge cycles.

Sealed AA size batteries of 1000 mAh were fabricated by assembling a hydrogen-absorbing alloy electrode as the negative electrode and a sintered nickel electrode as the positive electrode. Instead of sintered nickel electrode, a non-sintered nickel electrode was used, and AA size batteries of 1500 and 1700 mAh were also fabricated and used for the test. They were charged at 0.1 C for 16 h and discharged at 1 C until cell voltage reached 1.0 V at room temperature; this charge/discharge cycle was repeated three times for initial activation.

Life tests were performed by charging the batteries at 1 C rate until battery voltage decreased 10 mV from the peak voltage and discharging them at 1 C rate until the voltage repeatedly reached 1.0 V at room temperature.

Degradation of the hydrogen-absorbing alloys after cycling was investigated by measuring their oxygen content and particle size. The oxygen content of the alloys was measured with an infrared absorption method using an LECO RQ-416DR oxygen analyzer. The density of the alloys was also measured with He gas substitution method using Shimadzu Accupyc 1330.

3. Results and discussion

3.1. Cycle characteristics of batteries using R–Mg–Ni alloys

First, we examined the cycle characteristics of AA size batteries using the previously reported $La_{0.7}Mg_{0.3}Ni_{3.3}$ and $La_{0.7}Mg_{0.3}Ni_{2.8}Co_{0.5}$ alloys [1] and the $MmNi_{3.3}Co_{0.8}Al_{0.2}Mn_{0.6}$ alloy that has already been used in commercial batteries. As shown in Fig. 2, the cycle life of AA size batteries using the $La_{0.7}Mg_{0.3}Ni_{3.3}$ and $La_{0.7}Mg_{0.3}Ni_{2.8}Co_{0.5}$ alloys was 30% and 70% shorter than batteries using the $MmNi_{3.3}Co_{0.8}Al_{0.2}Mn_{0.6}$ alloy, respectively. Note that even this level of Co substitution for Ni degraded the cycle characteristics, whereas Co substitution is indispensable for improving the cycle characteristics for Mm–Ni alloys with $CaCu_5$ structure [2–5].

Table 1 shows the oxygen content and particle size of the alloys before cycle and after 100 cycles. The oxygen content of the $La_{0.7}Mg_{0.3}Ni_{3.3}$ and $La_{0.7}Mg_{0.3}Ni_{2.8}Co_{0.5}$ alloys after 100 cycles was approximately two and three times higher than $MmNi_{3.3}Co_{0.8}Al_{0.2}Mn_{0.6}$, respectively, although the particle size of $La_{0.7}Mg_{0.3}Ni_{3.3}$ and $La_{0.7}Mg_{0.3}Ni_{2.8}Co_{0.5}$ alloys after 100 cycles was even bigger.

It is known that the oxidation of anode alloy shortens battery life. In these cycle tests, it was found that the failure

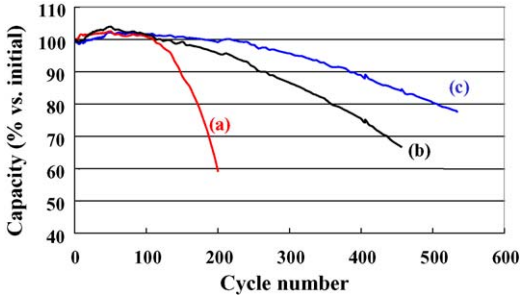

Fig. 2. Cycle behavior of 1000 mAh AA size cells using alloys: (a) $La_{0.7}Mg_{0.3}Ni_{2.8}Co_{0.5}$; (b) $La_{0.7}Mg_{0.3}Ni_{3.3}$; (c) $MmNi_{3.3}Co_{0.8}Al_{0.2}Mn_{0.6}$. Cycle condition: 1 C = 1000 mA; charge: 1 C, $-\Delta V$ (10 mV); discharge: 1 C, EV = 1.0 V; room temperature.

Table 1
Oxygen content and particle size before cycle and after 100 cycles

	Oxygen content (mass%)		Particle size (μm)
	Before cycle	After 100 cycles	After 100 cycles
$MmNi_{3.3}Co_{0.8}Al_{0.2}Mn_{0.6}$	0.33	1.15	19.4
$La_{0.7}Mg_{0.3}Ni_{3.3}$	0.68	1.99	23.4
$La_{0.7}Mg_{0.3}Ni_{2.8}Co_{0.5}$	0.92	3.30	20.0

Table 2
Oxygen content of $La_{0.7}Mg_{0.3}Ni_{3.2}M_{0.1}$ (M: Al, Mn) and $La_{0.7}Ni_{0.3}Ni_{3.3}$ alloys after 60 cycles in the three-electrode cell

	Oxygen content (mass%)
$La_{0.7}Mg_{0.3}Ni_{3.3}$	2.06
$La_{0.7}Mg_{0.3}Ni_{3.2}Al_{0.1}$	1.21
$La_{0.7}Mg_{0.3}Ni_{3.2}Mn_{0.1}$	1.77

mode of batteries using these R–Mg–Ni alloys after cycles was an increase in resistance due to separator dry up resulting from alloy oxidation. The reason for the shorter cycle life of the Co substituted alloy shown in Fig. 2 is considered to be the promotion of pulverization, judging from the change in particle size after cycles compared to the $La_{0.7}Mg_{0.3}Ni_{3.3}$ alloy.

3.2. Influence of substituting elements for nickel on cycle durability

We studied the influence of substituting elements for nickel on cycle durability. First, as has normally been done for superlattice alloys to improve their electrochemical characteristics, we examined the effect of aluminum and manganese substitutions. The oxygen content of the alloys substituted by aluminum and manganese after 60 charge/discharge cycles in a three-electrode test cell is shown in Table 2. Both aluminum and manganese substitutions suppressed oxidation, especially lowering the oxygen content of the $La_{0.7}Mg_{0.3}Ni_{3.2}Al_{0.1}$ alloy by 40% more than the $La_{0.7}Mg_{0.3}Ni_{3.3}$ alloy.

The effects of aluminum substitution were also confirmed in a cycle test in a 1500 mAh AA size battery, as shown in Fig. 3. Using the $La_{0.7}Mg_{0.3}Ni_{3.2}Al_{0.1}$ alloy, the cell's cycle life nearly doubled compared with the $La_{0.7}Mg_{0.3}Ni_{3.3}$ alloy. The change in the oxygen content of the $La_{0.7}Mg_{0.3}Ni_{3.2}Al_{0.1}$ and $La_{0.7}Mg_{0.3}Ni_{3.3}$ alloys during the cycle test is shown in Fig. 4. The oxygen content of the $La_{0.7}Mg_{0.3}Ni_{3.2}Al_{0.1}$ alloy after 150 cycles was even smaller than the $La_{0.7}Mg_{0.3}Ni_{3.3}$ alloy after 100 cycles, indicating that the improvement of the cycle life was due to the suppression of electrolyte consumption in the separator by using an alloy with higher oxidation

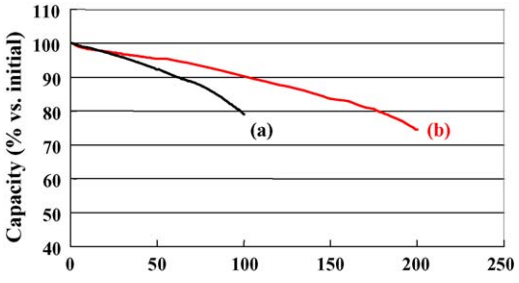

Fig. 3. Cycle behavior of 1500 mAh AA size cells using alloys: (a) $La_{0.7}Mg_{0.3}Ni_{3.3}$; (b) $La_{0.7}Mg_{0.3}Ni_{3.2}Al_{0.1}$. Cycle condition: 1 C = 1500 mA; charge: 1 C, $-\Delta V$ (10 mV); discharge: 1 C, EV = 1.0 V; room temperature.

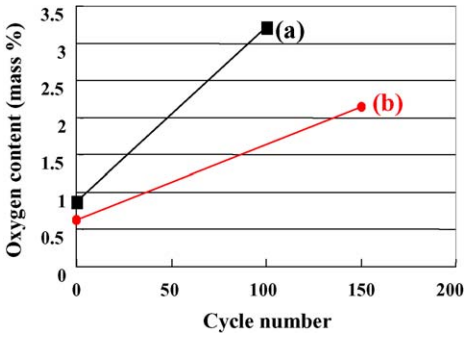

Fig. 4. Oxygen content of alloys: (a) $La_{0.7}Mg_{0.3}Ni_{3.3}$; (b) $La_{0.7}Mg_{0.3}Ni_{3.2}Al_{0.1}$.

resistibility. It is considered that a Ni-rich layer is effectively formed on the surface of the Al substituted alloy after the dissolution of Al into the electrolyte and works as a protection layer against the oxidation during cycles [6].

3.3. Optimization of magnesium content

To improve durability and reduce the cost of the $La_{0.7}Mg_{0.3}Ni_{3.2}Al_{0.1}$ alloy, La was replaced by Mm, and Al content was increased from 0.1 to 0.2. Magnesium content was optimized for this alloy. By changing the magnesium content from $x = 0.17$–0.30 in $Mm_{1-x}Mg_xNi_{3.1}Al_{0.2}$, the cycle life of 1500 mAh AA size batteries using these alloys was examined. Cycle life was prolonged by decreasing the magnesium content, as shown in Fig. 5. The cycle life for $x = 0.17$ was 2.5 times longer than $x = 0.30$. The oxygen content of the $Mm_{1-x}Mg_xNi_{3.1}Al_{0.2}$ alloys accordingly decreased with a decrease of magnesium content. Since particle size increased with a decrease in magnesium content, as also shown in Fig. 6, the oxidation of the alloys was considered suppressed because of the suppressed pulverization for lower magnesium content. Since little difference existed in the oxygen content between $x = 0.17$ and 0.20, from the viewpoint of cycle durability, optimal magnesium content was considered to be in the range of $x = 0.17$–0.20.

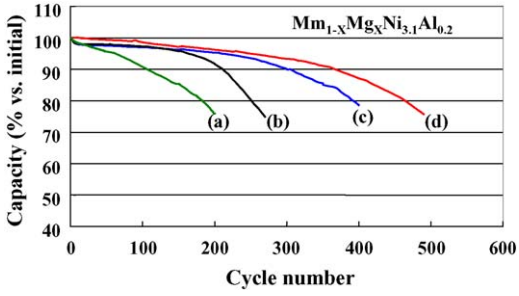

Fig. 5. Cycle behavior of 1500 mAh AA size cells using $Mm_{1-x}Mg_xNi_{3.1}Al_{0.2}$ alloys. (a) $x = 0.30$; (b) $x = 0.25$; (c) $x = 0.20$; (d) $x = 0.17$. Cycle condition: 1 C = 1500 mA; charge: 1C, $-\Delta V$ (10 mV); discharge: 1 C, EV = 1.0 V; room temperature.

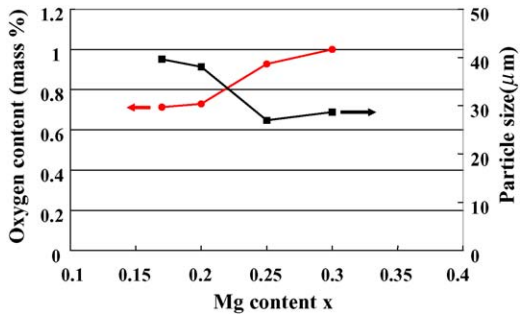

Fig. 6. Oxygen content and particle size of $Mm_{1-x}Mg_xNi_{3.1}Al_{0.2}$ alloys after 100 cycles.

The cycle characteristics of the 1700 mAh cells using the $Mm_{0.83}Mg_{0.17}Ni_{3.1}Al_{0.2}$ alloy and the $MmNi_{3.3}Co_{0.8}Al_{0.2}Mn_{0.6}$ alloy with $CaCu_5$ structure, which has already been used for commercialized cells, were compared in Fig. 7. The cycle life of the cell using the $Mm_{0.83}Mg_{0.17}Ni_{3.1}Al_{0.2}$ alloy was improved by approximately 30% compared with the $MmNi_{3.3}Co_{0.8}Al_{0.2}Mn_{0.6}$ alloy. The $Mm_{0.83}Mg_{0.17}Ni_{3.1}Al_{0.2}$ alloy showed 10% larger discharge capacity than the $MmNi_{3.3}Co_{0.8}Al_{0.2}Mn_{0.6}$ alloy, demonstrating larger capacity and longer cycle life of the developed superlattice alloy than conventional alloys with $CaCu_5$ structure.

3.4. Crystal structure of $Mm_{0.83}Mg_{0.17}Ni_{3.1}Al_{0.2}$ alloy

The crystal structure of the $Mm_{0.83}Mg_{0.17}Ni_{3.1}Al_{0.2}$ alloy was investigated using powder X-ray diffractometry (XRD). The measured XRD profile was shown in Fig. 8 together with that of the $MmNi_{3.3}Co_{0.8}Al_{0.2}Mn_{0.6}$ alloy. The XRD profile of the $Mm_{0.83}Mg_{0.17}Ni_{3.1}Al_{0.2}$ alloy was quite different from the $CaCu_5$ structure and was identified with the Ce_2Ni_7 structure. The lattice constant of $Mm_{0.83}Mg_{0.17}Ni_{3.1}Al_{0.2}$ alloy was calculated to be $a = 0.502$ nm and $c = 2.442$ nm. The length of the a-axis is almost the same as the $MmNi_{3.3}Co_{0.8}Al_{0.2}Mn_{0.6}$ alloy ($a = 0.503$ nm and $c = 0.405$ nm), and the length of the c-axis is approximately six times longer. The crystal structure of the

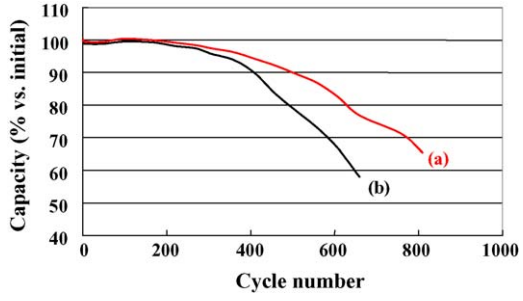

Fig. 7. Cycle behavior of 1700 mAh AA size cells using alloys: (a) $Mm_{0.83}Mg_{0.17}Ni_{3.1}Al_{0.2}$; (b) $MmNi_{3.3}Co_{0.8}Al_{0.2}Mn_{0.6}$. Cycle condition: 1 C = 1700 mA; charge: 1 C, $-\Delta V$ (10 mV); discharge: 1 C, EV = 1.0 V; room temperature.

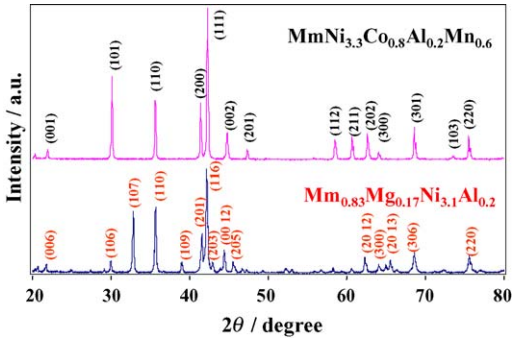

Fig. 8. XRD profiles of $Mm_{0.83}Mg_{0.17}Ni_{3.1}Al_{0.2}$ and $MmNi_{3.3}Co_{0.8}Al_{0.2}Mn_{0.6}$ alloys.

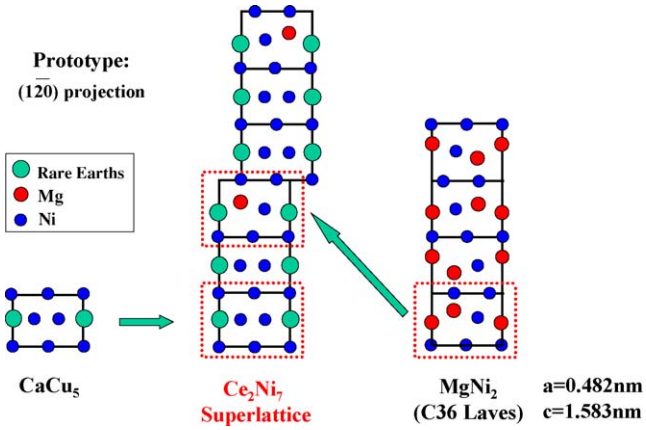

Fig. 9. Crystal structure of $Mm_{0.83}Mg_{0.17}Ni_{3.1}Al_{0.2}$ alloy.

$Mm_{0.83}Mg_{0.17}Ni_{3.1}Al_{0.2}$ alloy, illustrated in Fig. 9, consists of two different subcells: one is the $CaCu_5$ subcell and the other is part of the $MgNi_2$ C36 Laves-type unit cell. Since the $CaCu_5$ subcell of the $Mm_{0.83}Mg_{0.17}Ni_{3.1}Al_{0.2}$ alloy is nearly as big as the unit cell of the $MmNi_{3.3}Co_{0.8}Al_{0.2}Mn_{0.6}$ alloy, the larger hydrogen capacity of the $Mm_{0.83}Mg_{0.17}Ni_{3.1}Al_{0.2}$ alloy can probably be attributed to the Mg containing the subcell. Such further structure refinement to identify the Al occupying site will be conducted in the future.

Note also that the density of the $Mm_{0.83}Mg_{0.17}Ni_{3.1}Al_{0.2}$ alloy was measured to be 8.05 g cm^{-3}, which is nearly the same as commercialized Mm–Ni alloys with $CaCu_5$ structure. From a practical point of view, this is important since larger gravimetric hydrogen capacity can be effectively utilized to increase battery capacity with restricted volume.

4. Conclusions

The cycle durability of R–Mg–Ni (R: rare earths) superlattice alloys has been improved by partly substituting Al for Ni and optimizing Mg content. The improved $Mm_{0.83}Mg_{0.17}Ni_{3.1}Al_{0.2}$ alloy with Ce_2Ni_7 structure eventually possesses better cycle durability and higher electrochemical capacity than conventional Mm–Ni alloys with $CaCu_5$

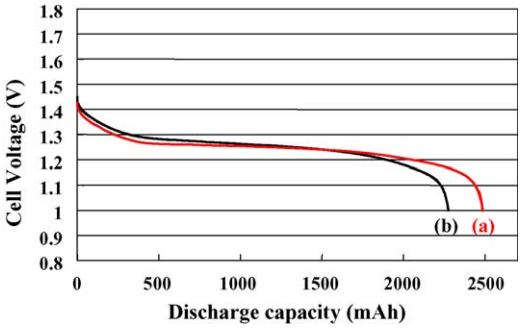

Fig. 10. Discharge curves of AA size cells: (a) Ni-MH 2500 using Mm–Mg–Ni superlattice alloy; (b) Ni-MH 2300 using Mm–Ni alloy with $CaCu_5$ structure. Test condition—charge: 250 mA × 16 h; discharge: 500 mA, EV = 1.0 V; room temperature.

structure. Using a further improved superlattice alloy, new Ni-MH batteries for the retail market, the Ni-MH 2500/900 series (AA size type 2500 mAh; AAA size type 900 mAh), have been developed and commercialized. The new model has been designed to maximize the performance of high-capacity superlattice alloys and exhibits a larger capacity of 200 mAh than the previous model Ni-MH2300 using a conventional Mm–Ni alloy, as shown in Fig. 10. These new R–Mg–Ni superlattice alloys are expected to open up the possibilities of further improvements in Ni-MH batteries.

References

[1] T. Kohno, H. Yoshida, F. Kawashima, T. Inaba, I. Sakai, M. Yamamoto, M. Kanda, J. Alloys Compd. 311 (2000) L5–L7.
[2] A. Züttel, D. Chartouni, K. Gross, P. Spatz, M. Bächler, F. Lichtenberg, A. Fölzer, N.J.E. Adkins, J. Alloys Compd. 626 (1997) 253–254.
[3] N. Higashiyama, Y. Matsuura, H. Nakamura, M. Kimoto, M. Nogami, I. Yonezu, K. Nishio, J. Alloys Compd. 648 (1997) 253–254.
[4] K. Inoue, T. Matsumoto, S. Kameoka, N. Furukawa, Sanyo Tech. Rev. 20 (3) (1988) 86–95.
[5] T. Sakai, T. Hazama, H. Miyamura, N. Kuriyama, A. Kato, H. Ishikawa, J. Less-common Met. 172–174 (1991) 1175–1184.
[6] F. Meli, L. Schlapbach, J. Less-Common Met. 172–174 (1991) 1252–1259.